Cobalt(II) and copper(II) supramolecular networks with 1-iminoisoindoline asymmetric pincer

Piotr Zabierowski, Dariusz Matoga, * Wojciech Nitek

SUPPLEMENTARY INFORMATION

List of figures:

List of tables:

Discussion of hydrogen bonding in 1 and 2

In complex **1** the *cis*-coordinated chlorido ligands are closer to each other than in complex **2** (the Cl1-M1-Cl2 angles are 110.1° for **1** and 122.7° for **2**). As a result of this steric crowding the number of hydrogen bonds in which Cl acceptors participate is lower in comparison with the crystal lattice of **2**. In the case of **1**, only two types of hydrogen bonds can be distinguished, when the following criteria are taken: H···A distance < 3.0Å and DHA angle > 120° (Fig. S2A). These hydrogen bonds, with D···A distances in between 3.6-3.7 Å, exist: (i) between the axial Cl1 ligand and iminoisoindoline sp^2 C2 pirydyl carbon donor; (ii) between Cl2 and sp^3 C15 picolyl carbon donor. These weak lattice forces contribute to a formation of infinite chains propagating along the *c* axis (see Fig. S2B) which are stacked together by relatively strong π-π interactions between the iminopicolinic pirydyl rings in a parallel offset manner (centroid···centroid distance is 3.9 Å and the distance between parallel ring planes is 3.3 Å) . The graph set analysis of hydrogen bonds for **1** (Fig. S1) shows the presence of two types of ring motifs in the crystal lattice. No empty space is observed in the crystal structure of **1** (Fig. S2C). In the case of complex **2**, the hydrogen bond network is more diversified than in **1**, what is shown in Fig. 2A. A total number of four types of weak hydrogen bonds may be distinguished (with D···A distances close to 3.6 Å), in the crystal lattice of **2**, which contribute to a formation of nine ring motifs shown in graph set analysis of hydrogen bonds in **2** (Fig. S3). Three of them exist between Cl1 and (i) isoindoline sp^3 C14, (ii) isoindoline sp^2 C11, (iii) iminopicolinic pirydyl sp^2 C3. Another hydrogen bond occurs between Cl2 and sp^2 C17 of the *N*-picolyl part of the *pap* ligand. The aforementioned hydrogen bonds construct a three-dimensional supramolecular network together with strong π-π interactions between iminoisoindoline parts of the pap ligands (Fig. 2B). Contrary to the structure of **1**, empty cavities may be observed in the crystal lattice of **2** as channels (approx. 4.4 x 4.5 Å2) along the *a* axis (Fig. 3C). In spite of that, however, the closest intermetallic non-bonding distance for **2** (6.795 Å) is smaller than that for **1** (8.221 Å).

*Table S1. Crystallographic parameters for **3** and **4**. The estimated standard deviations are shown in round brackets.*

compound	**3**	**4**
chemical formula	$C_{56}H_{78}Cu_2N_8O_{26}$	$C_{56}H_{78}Co_2N_4O_{26}$
formula weight	1406.34	1397.12
a [Å]	11.6680(2)	11.6110(2)
b [Å]	11.9800(2)	12.0270(3)
c [Å]	13.5510(2)	13.7710(3)
α	110.919(1)°, 107.137(1)°, 100.586	111.188(1)°, 107.070(1)°, 102.238(1)°
β	(1)°	
γ		
μ [mm^{-1}]	0.75	0.61
V [$Å^3$]	1599.77(5)	1601.22(6)
Z	2	2
Space group	*P*-1	*P*-1
T [K]	100	100
λ [Å]	0.71069	0.71069
D_{calc} [g cm^{-3}]	1.461	1.451
$R[F^2 > 2\sigma(F^2)]$[a]	0.031	0.031
$wR(F^2)$[a]	0.079	0.078

[a] Parameters definition: $R=\Sigma(|F_o|-|F_c|)/\Sigma(|F_o|)$; $wR(F^2)=\{\Sigma[w(F_o^2-F_c^2)^2\}^{1/2}$; $w=1/[\sigma^2(F_o^2)+(0.0808P)^2 + 2.6927P]$; $P = (F_o^2 + 2F_c^2)/3$

*Table S2. Crystallographic parameters for **5**. The estimated standard deviations are shown in round brackets.*

chemical formula	$C_{24}H_{27.2}CoN_4O_{6.6}$
formula weight	536.23
a [Å]	10.8607(4)
b [Å]	10.3695(5)
c [Å]	20.7248(9)
α	90°
β	96.103(3)°
γ	90°
μ [mm^{-1}]	0.792
V [$Å^3$]	2320.80(17)
Z	4
Space group	$P2_1/c$
T [K]	120(2)
λ [Å]	0.71073
D_{calc} [g cm^{-3}]	1.535
$R[F^2 > 2\sigma(F^2)]$[a]	0.0541
$wR(F^2)$[a]	0.1214

[a]Parameters definition: $R=\Sigma(|F_o|-|F_c|)/\Sigma(|F_o|)$; $wR(F^2)=\{\Sigma[w(F_o^2-F_c^2)^2\}^{1/2}$; $w=1/[\sigma^2(F_o^2)+(0.0808P)^2 + 2.6927P]$; $P = (F_o^2 + 2F_c^2)/3$

Comments on the refinement process of 5

The disorder in succinate moiety was treated in the following way: (i) all atomic positions for the bridging succinate ligand were split, (ii) occupation in these positions were assumed as 2:1 rather than 1:1. Additionally, the disorder in the crystallization water molecules was modeled by splitting O6 atom to O(6A), O(6B) and O(6C). Only one of these three positions can be occupied in each unit cell, hence the sum of the occupancies of the three positions cannot be larger than 1. The best fit was obtained assuming 1.6 molecules of disordered H_2O (or 2.6 H_2O total) per formula unit. The hydrogen atoms of the disordered water molecules (1.6 H_2O) were not included in the refinement and thus the formula sum differs from the one proposed based on elemental analysis results. Some of the non-hydrogen atoms in the main residue were refined isotropically in order to enhance the convergence. The freshly synthesized sample of **5** contains five crystallization water molecules as calculated from TGA analysis (see Fig. S7).

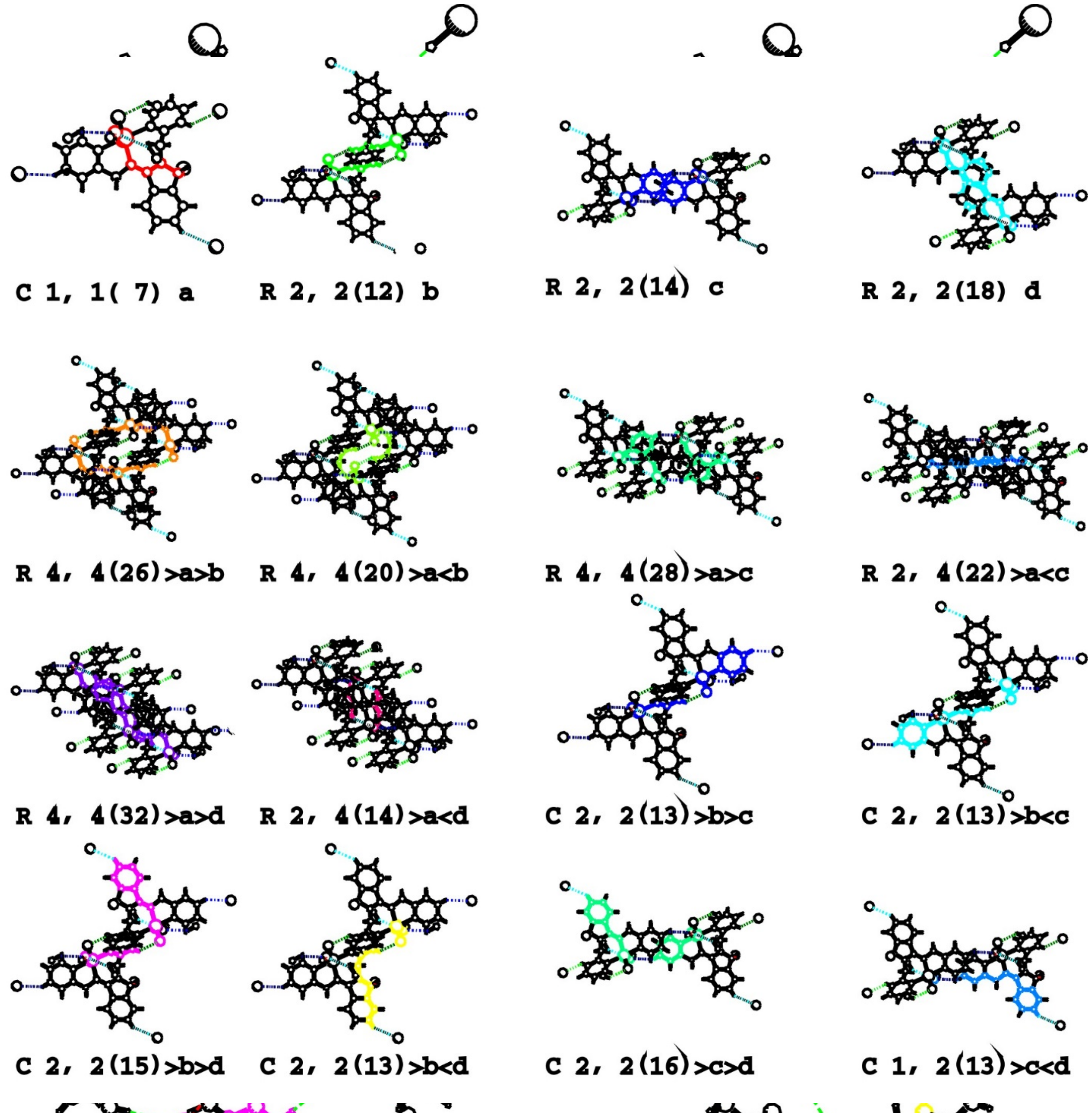

*Figure S2. Graph sets analysis of hydrogen bonding in **2**.*

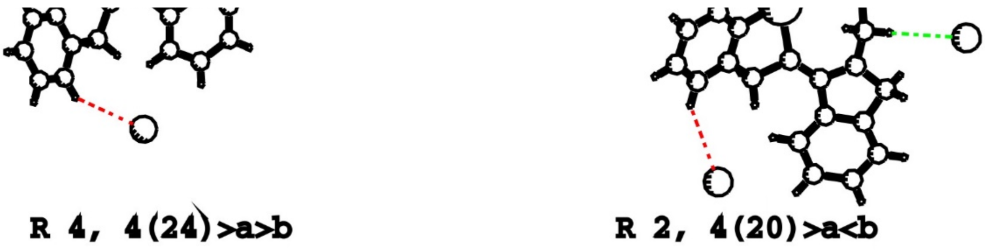

*Figure S1. Graph set analysis of hydrogen bonding in **1**.*

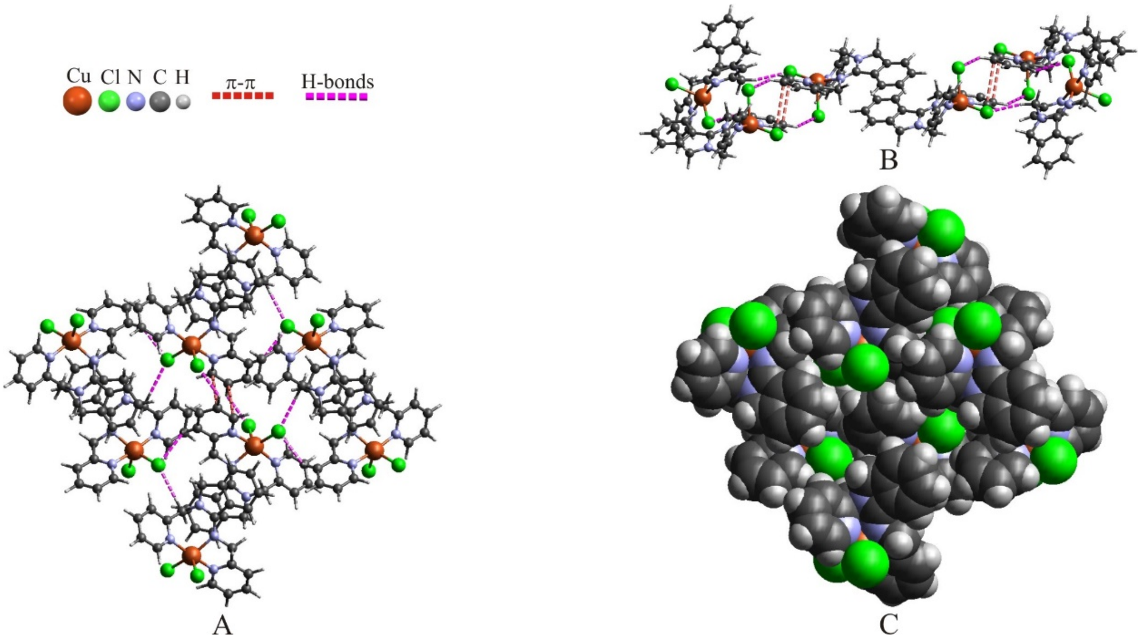

Figure S3. Crystal-packing interactions in the lattice of ***1****: Hydrogen bonds and π-π stacking interactions (A). Supramolecular chains along the c direction (B). Spacefill representation showing the absence of cavities (C).*

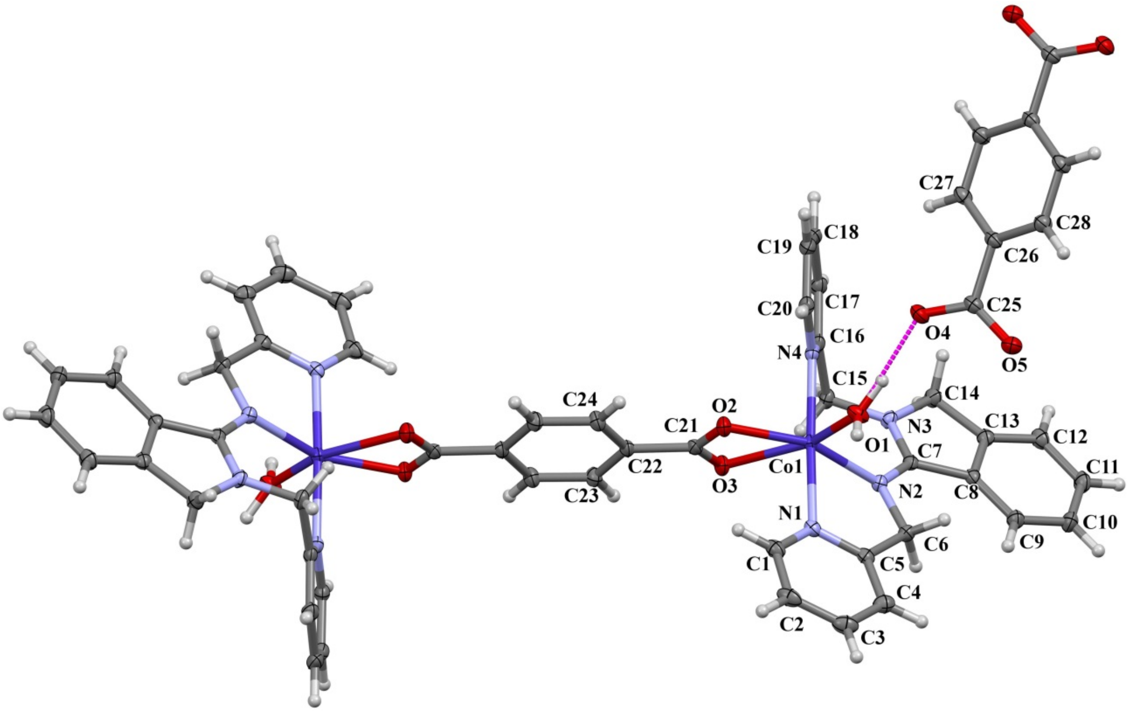

*Figure S4. The molecular structure of {[Co(H_2O)(pap)]$_2$(μ-ta)}·ta (**4**) together with atom labeling scheme. The crystallization water molecules were omitted for clarity.*

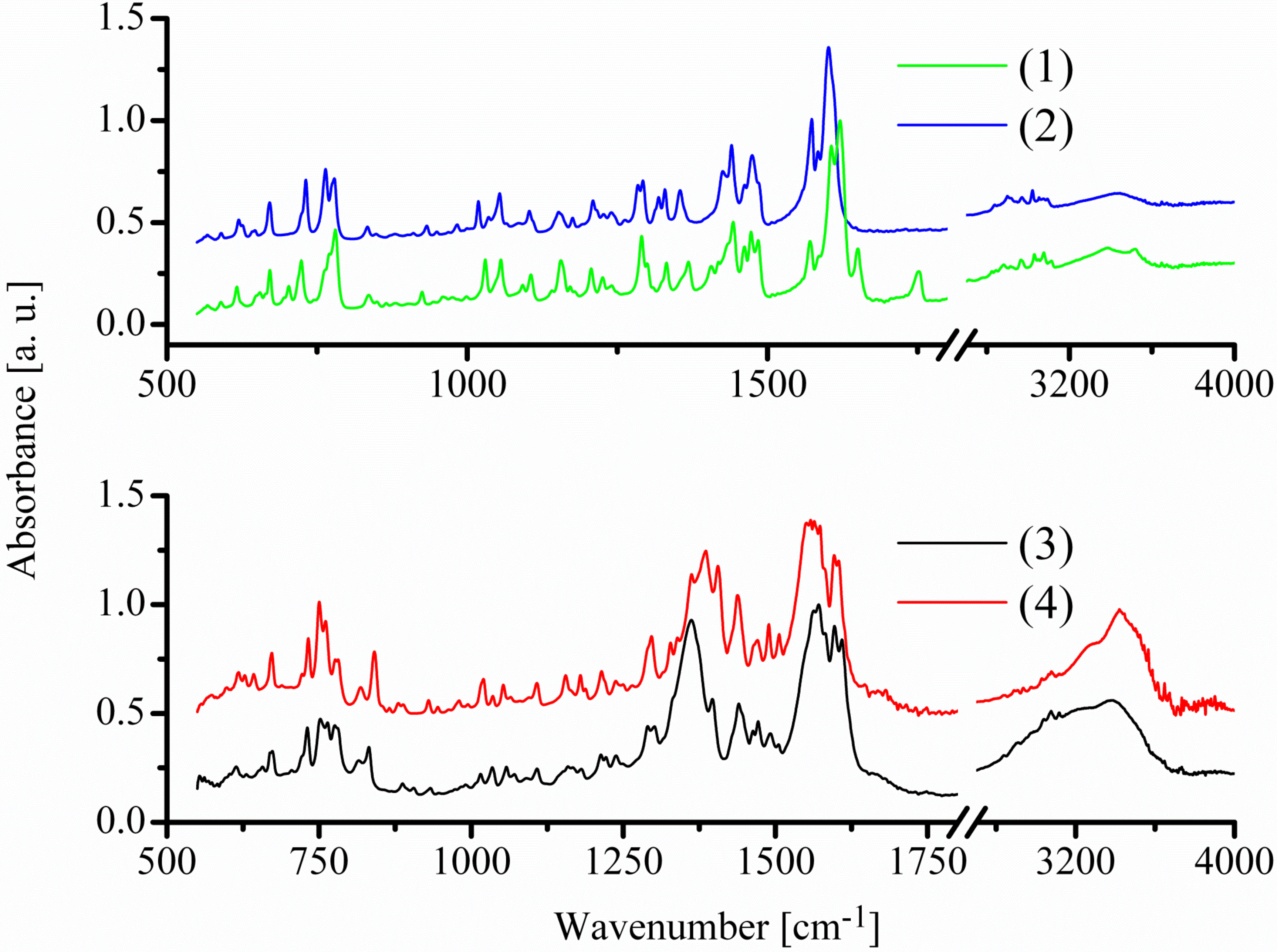

*Figure S5. The ATR FT IR spectra of **1-4**.*

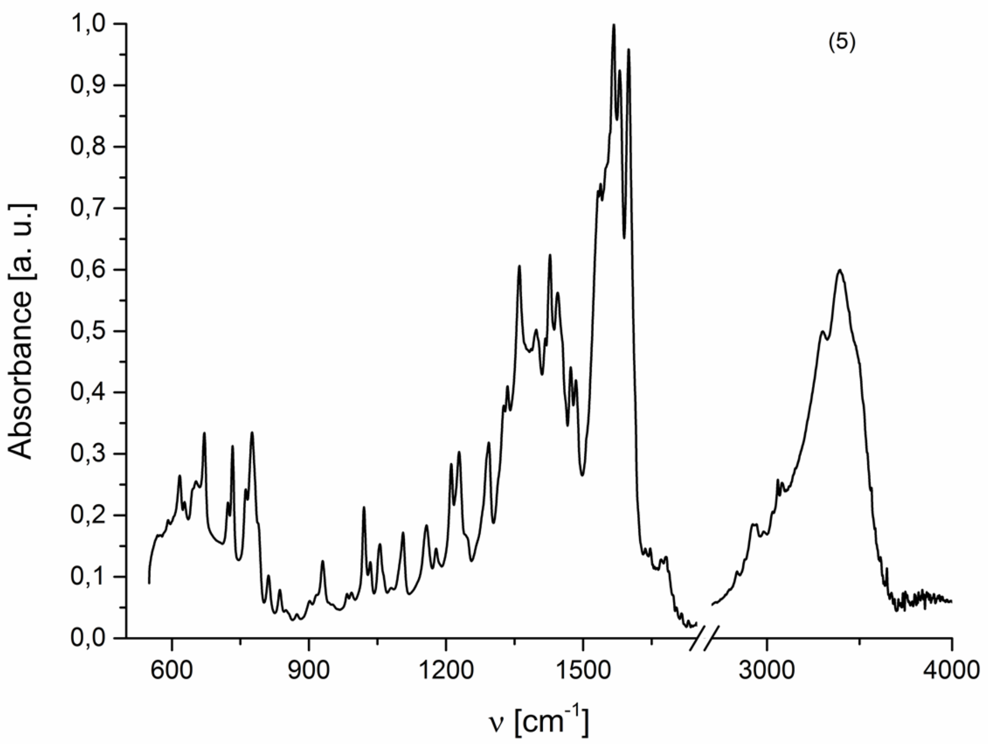

*Figure S6. The ATR FT IR spectrum of **5**.*

*Table S3. Conductivity measurements for **1** and **2** in aqueous solutions at 23.4 ^{o}C.*

Complex	*c* [mol/dm^3]	*L* [S]	κ [S/m]	Λ_m [S·m^2·mol^{-1}]
1	2,9E-03	6,6E-04	4,7E-02	1,6E-02
	1,8E-03	3,9E-04	2,7E-02	1,6E-02
	2,9E-04	6,3E-05	4,4E-03	1,5E-02
2	2,8E-03	6,3E-04	4,5E-02	1,6E-02
	2,8E-04	7,8E-05	5,5E-03	2,0E-02
	1,4E-04	4,3E-05	3,0E-03	2,1E-02

Legend: *c* – concentration; *L* – conductivity; κ – specific conductivity; Λ_m - molar conductivity

Comment:

The complexes **1** and **2** are electrolytes in aqueous solution. The molar conductivities depend on concentrations of the complexes.

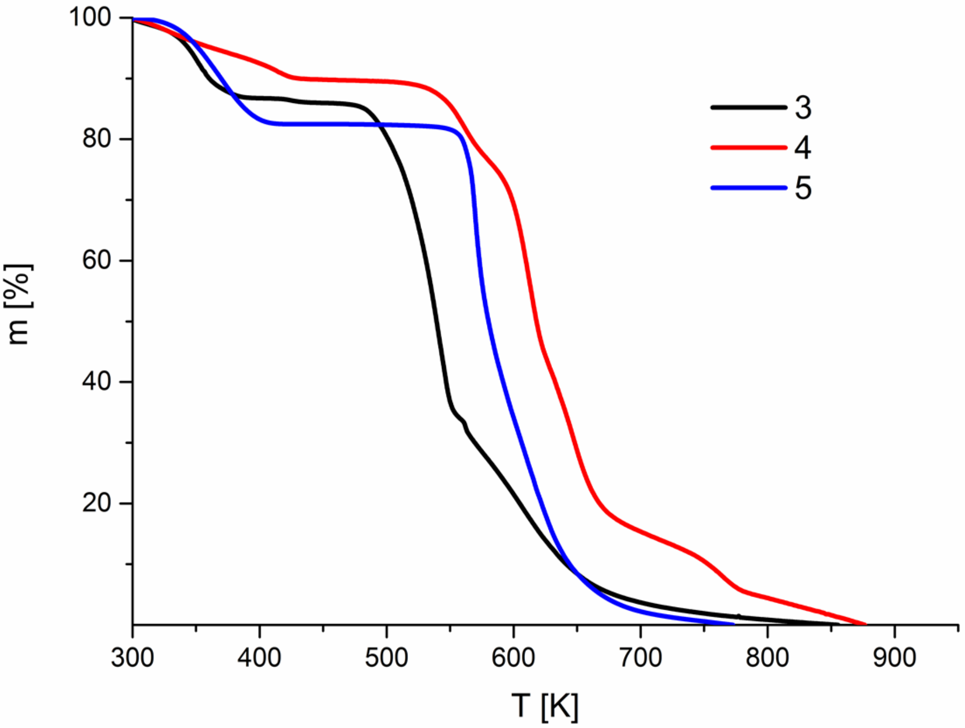

*Figure S7. Thermogravimetric analysis results for **3-5**.*

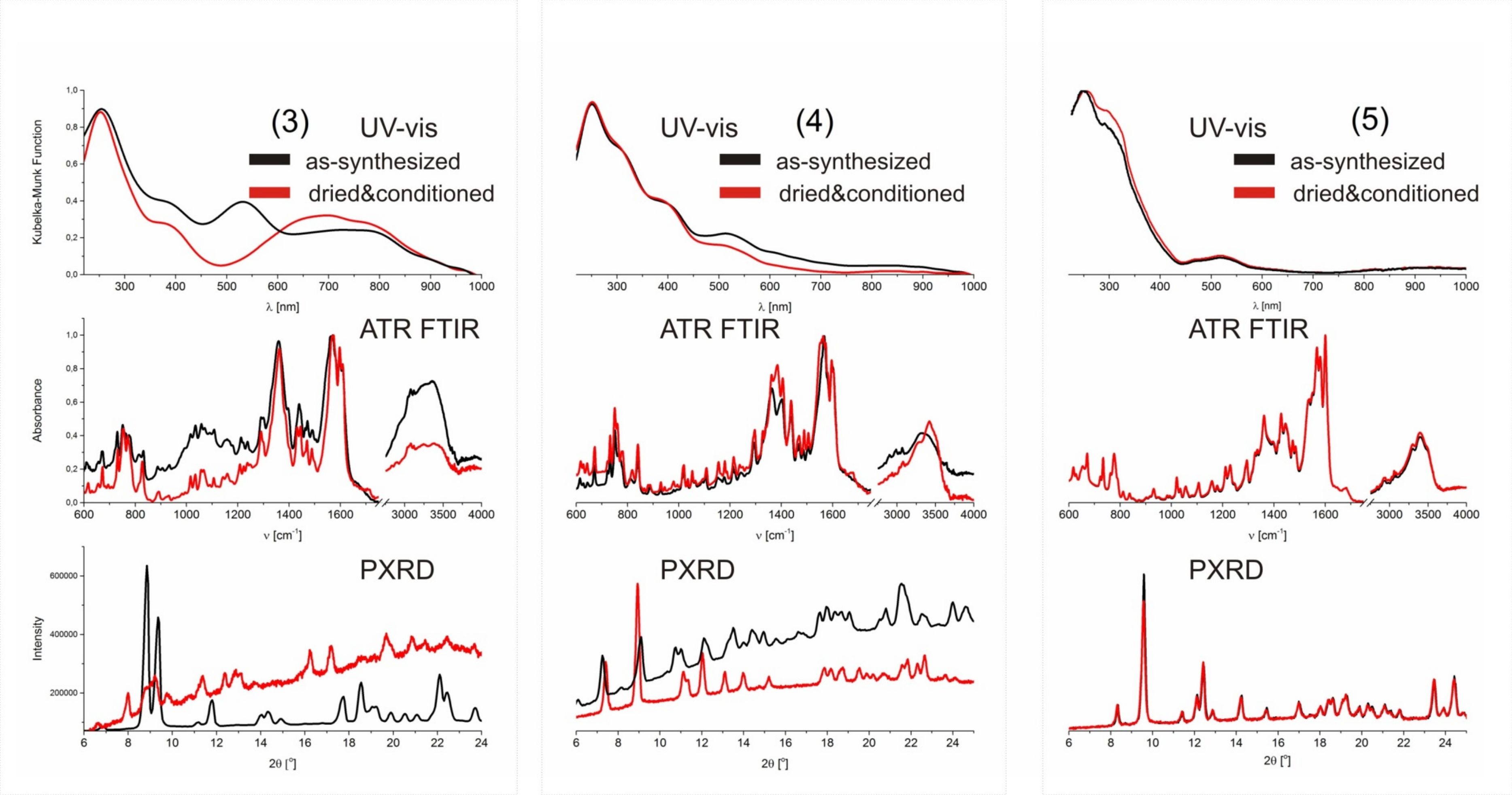

*Figure S8. Dehydration studies for **3-5**.. Dehydration conditions: 373 K, 50 mBar, 1h (**3** and **4**) and 393 K, 50 mBar, 40 min (**5**). After dehydration the samples were conditioned in air for 2h at 293 K prior to measurements.*